# A Model of the Post-Saccadic Dynamics of Visual Sensitivity

Bin Yang[1,2], Michele A Cox[1,2], Yuanhao Li[1,2], Scott Murdison[3], Zhetuo Zhao[1,2], Janis Intoy[2,4], Michele Rucci[1,2]

[1]Department of Brain and Cognitive Sciences, [2]Center for Visual Science, University of Rochester, USA
[3]Facebook Reality Labs, USA
[4]Graduate Program for Neuroscience, Boston University, USA

## Introduction

- Humans explore visual scenes by continually alternating rapid gaze shifts (saccades) with slow eye movements (ocular drifts);
- During viewing of natural scenes, this behavior yields a luminance flow with equalized power within an oscillating bandwidth [1].

**What are the consequences of this luminance flow on visual sensitivity?**

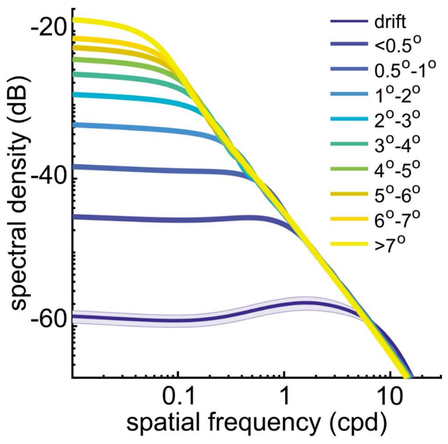


- We investigated this question by simulating the responses of retinal ganglion cells (RGC) at various eccentricities during the natural saccade/fixation cycle;
- We assume cell responses to be entirely driven by these transients (no sensitivity at 0 Hz).

## Model

### Visual Input

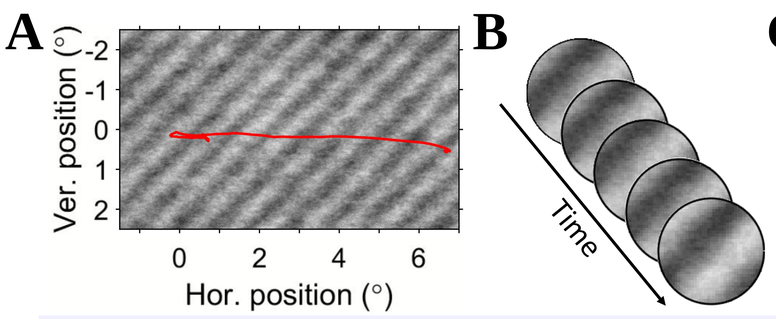


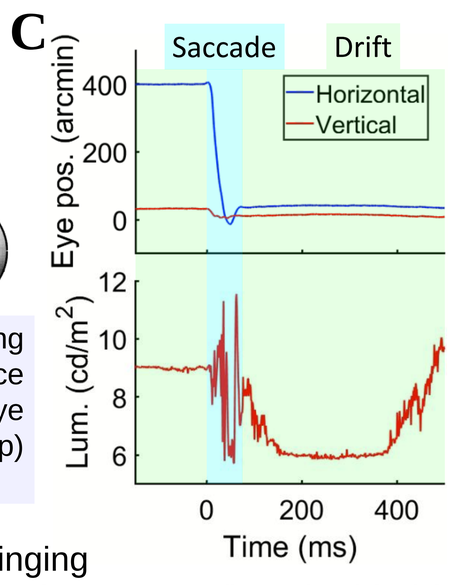


Retinal input during the saccade/drift cycle. ***A***, A grating embedded in natural noise with an example eye trace on top (red). ***B***, The retinal image moves due to eye movements. ***C***, the same eye trace shown in ***A*** (top) and the resulting luminance flow (bottom).

- We reconstructed the luminance signals impinging onto the retina as humans detected gratings (2 or 10 cpd) embedded in natural noise fields.
- Saccades resulted in abrupt changes in luminance, whereas drifts introduced slow modulations.

### Retinal Responses

- We modeled ON and OFF, parvo and magno cells as rectified spatiotemporal filters with parameters from neurophysiological data [2-4];
- RGC mosaics followed cell density maps from anatomical data [5-8].

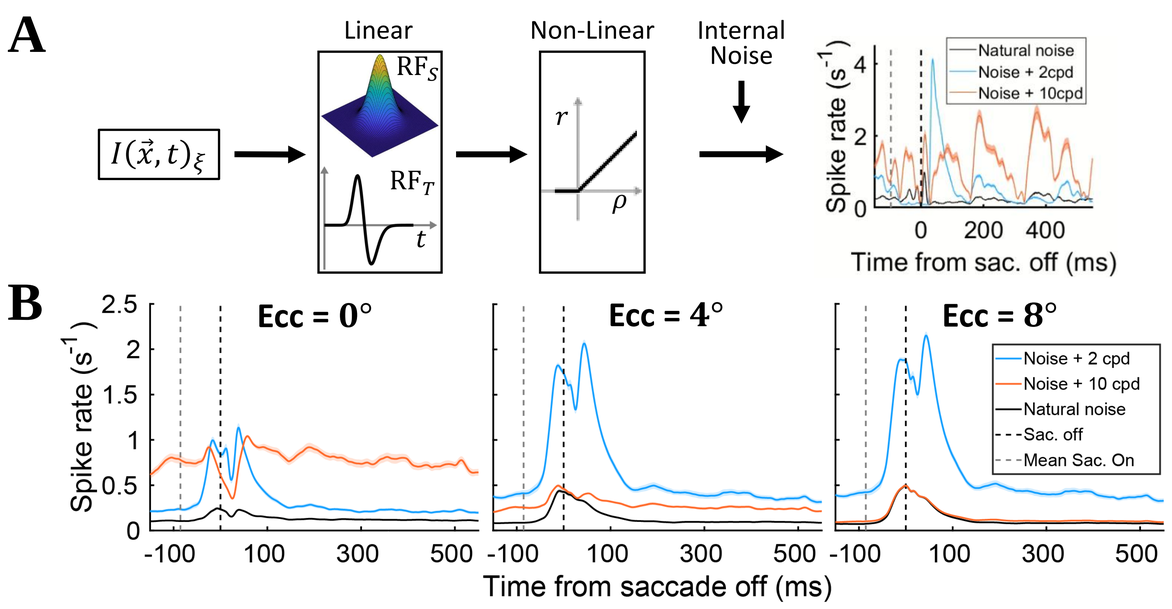


***A***, Retinal ganglion cells (RGCs) were models as rectified linear filters with separable spatial ($\mathrm{RF}_S$ [2]) and temporal ($\mathrm{RF}_T$ [3,4]) kernels. $I(\vec{x},t)_\xi$represents the luminance flow given the eye trace $\xi$. ***Right***, Average responses of parvo On cells given an example eye trace. ***B***, Average responses of all cells across eccentricities. Shaded regions, SEM across trials.

## Conclusions

- A biologically-plausible model that encodes space from oculomotor-induced temporal modulations closely replicates human dynamics of contrast sensitivity across the visual field;
- Sensitivity to low spatial frequencies is primarily determined by the fast input changes caused by saccades;
- Sensitivity to high spatial frequencies increases during post-saccadic fixation because of the transients from eye drifts.

### Detection

- To determine whether a grating was present, the integrated post-saccadic mean activity across all cells ($\overline{r_i}(t)$) at a given eccentricity was compared to a threshold ($\gamma(t)$).

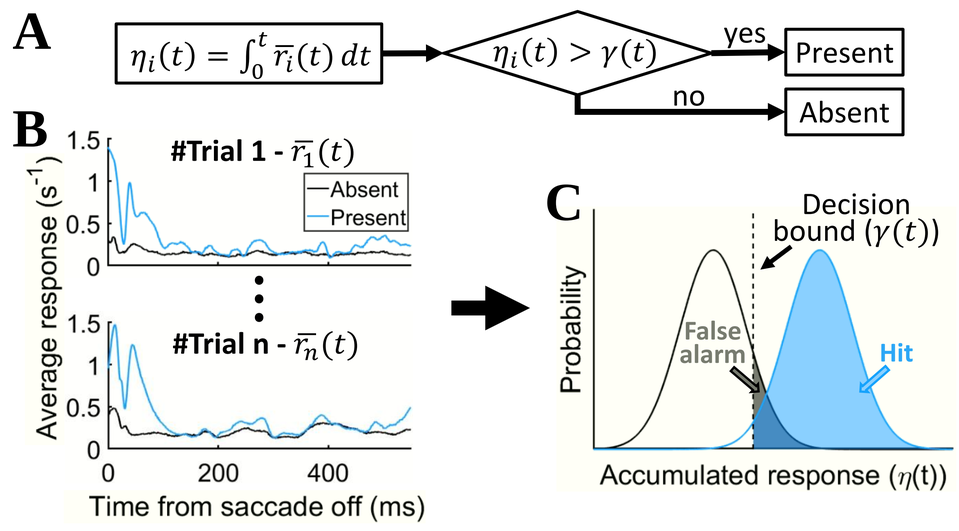


Detection stage. ***A***, For a given trial $i$, the average response across all cells ($\overline{r_i}(t)$) is integrated from saccade off ($\eta_i(t)$). The model reports presence of the grating if $\eta_i(t) > \gamma(t)$. ***B***, Mean activity across all cells for example trials. ***C***, Distributions of integrated responses in the presence (blue) and absence (black) of the grating.

## Results

### Contrast Sensitivity

- For a 2-cpd grating, contrast sensitivity saturates immediately after a saccade and does not increase with further exposure;
- For a 10-cpd grating, contrast sensitivity increases with prolonged post-saccadic exposure time;
- These dynamics closely replicate experimental data (see poster #1930).

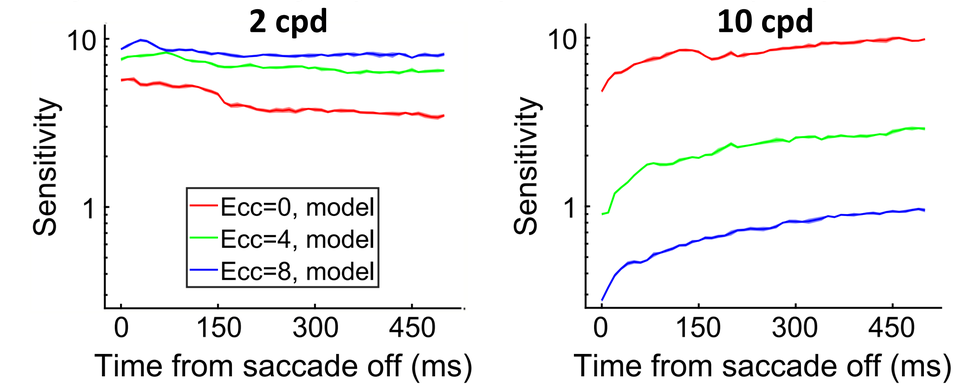


Contrast sensitivity predicted by the model at 2 cpd (***left***) and 10 cpd (***right***). Shaded regions represent $\pm 1\mathrm{s.e.}$.

### Control Oculomotor Transients

- Eliminating saccadic transients strongly impairs sensitivity at 2 cpd;
- Eliminating drift modulations impairs the increment in sensitivity at 10 cpd during post-saccadic fixation.

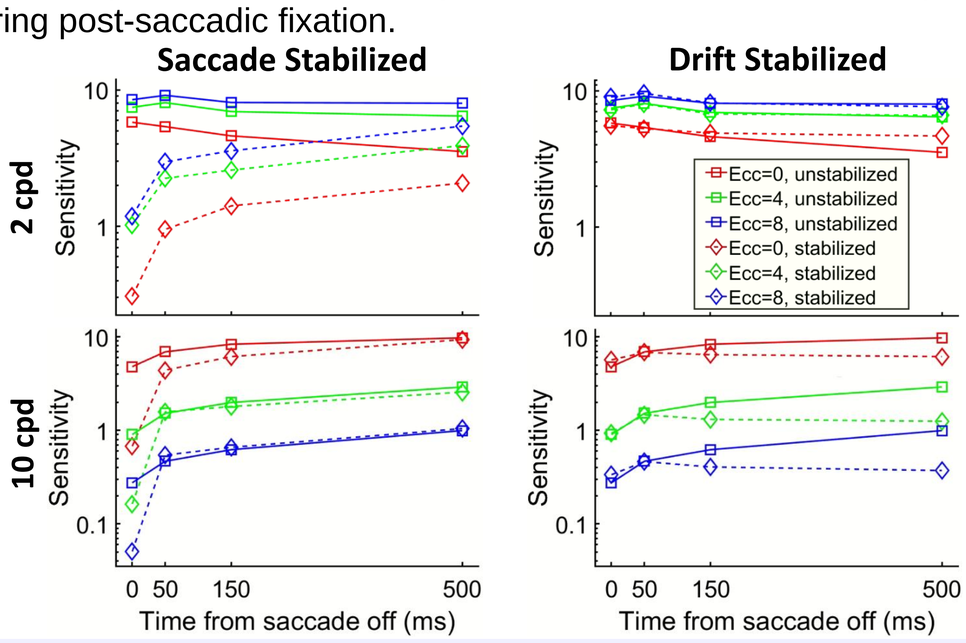


Comparison of contrast sensitivity between unstabilized and stabilized conditions. ***Left***, saccade stabilized; ***Right***, drift stabilized. ***Top***, 2 cpd; ***Bottom***, 10 cpd.

## Reference

[1] Mostofi, N., Zhao, Z., Intoy, J., Boi, M., Victor, J. D., & Rucci, M. (2020). Spatiotemporal Content of Saccade Transients. Current Biology, 30(20), 3999-4008.
[2] Croner, L. J., & Kaplan, E. (1995). Receptive fields of P and M ganglion cells across the primate retina. Vision research, 35(1), 7-24.
[3] Benardete, E. A., & Kaplan, E. (1997). The receptive field of the primate P retinal ganglion cell, I: Linear dynamics. Visual neuroscience, 14(1), 169-185.
[4] Benardete, E. A., & Kaplan, E. (1999). The dynamics of primate M retinal ganglion cells. Visual neuroscience, 16(2), 355-368.
[5] Watson, A. B. (2014). A formula for human retinal ganglion cell receptive field density as a function of visual field location. Journal of vision, 14(7), 15-15.
[6] Drasdo, N., Millican, C. L., Katholi, C. R., & Curcio, C. A. (2007). The length of Henle fibers in the human retina and a model of ganglion receptive field density in the visual field. Vision research, 47(22), 2901-2911.
[7] Dacey, D. M., & Petersen, M. R. (1992). Dendritic field size and morphology of midget and parasol ganglion cells of the human retina. Proceedings of the National Academy of sciences, 89(20), 9666-9670.
[8] Cottaris, N. P., Jiang, H., Ding, X., Wandell, B. A., & Brainard, D. H. (2019). A computational-observer model of spatial contrast sensitivity: Effects of wave-front-based optics, cone-mosaic structure, and inference engine. Journal of vision, 19(4), 8-8.

## Acknowledgement

Facebook Reality Labs; National Institutes of Health grants EY018363 (MR) and EY029565 (JI).